Article

Discovery Medicine 2025; 37(201): 2309–2319
https://doi.org/10.24976/Discov.Med.202537201.196

TSP-1 Promotes Bone Healing via Angiogenesis and MSC Recruitment in Rat Fractures

Chengbo Wu[1], Xing Lu[2], Xiliang Zang[3,*]

[1]Department of Trauma II, Yantaishan Hospital, 264001 Yantai, Shandong, China
[2]Department of Trauma I, Yantaishan Hospital, 264001 Yantai, Shandong, China
[3]Department of Trauma Microsurgery, The 970th Hospital of the Joint Logistics Support Force of The Chinese People's Liberation Army, 264000 Yantai, Shandong, China
*Correspondence: zangxiliang@163.com (Xiliang Zang)
Submitted: 11 July 2025 Revised: 22 July 2025 Accepted: 7 August 2025 Published: 20 October 2025

Background: Thrombospondin-1 (TSP-1) is a multifunctional glycoprotein involved in various physiological processes, including tissue repair and the regulation of angiogenesis. However, its role in bone regeneration remains unclear. This study aims to investigate the role of TSP-1 in promoting bone healing in a rat fracture model, with a particular focus on its effects on angiogenesis and the recruitment of mesenchymal stem cells (MSCs).

Methods: A stable femoral fracture model was established in rat. The experimental rat received treatment of TSP-1, MSCs, or a combination of both, and bone healing was assessed 2 weeks post-surgery. Micro-computed tomography (micro-CT) was used to evaluate bone regeneration by analyzing bone mineralization and trabecular parameters. Immunohistochemistry was performed to detect angiogenesis and bone formation markers (Cluster of Differentiation 105 (CD105), Cluster of Differentiation 31 (CD31), Bone Morphogenetic Protein-2 (BMP-2)). To investigate the mechanism by which TSP-1 promotes angiogenesis, 5-ethynyl-2′-deoxyuridine staining (EdU) staining was used to assess endothelial cell proliferation, and Western blotting was conducted to measure the protein expression of cyclooxygenase-2 (COX-2) and vascular endothelial growth factor (VEGF). A tube formation assay was used to evaluate the effect of TSP-1 on endothelial cell tube formation. Additionally, MSCs were co-cultured with TSP-1 for 7 days, and Transwell migration assays were performed to evaluate MSC migration. Tube formation assays were also used to assess vascular differentiation potential of MSCs. Immunofluorescence staining was performed to detect the expression of endothelial cell markers CD31, vascular endothelial growth factor receptor 1 (VEGFR1), and vascular endothelial growth factor receptor 2 (VEGFR2) in MSCs.

Results: Two weeks post-surgery, the TSP-1 and MSC groups exhibited significantly more callus, denser trabecular bone, and higher mineralization levels compared to the model group ($p < 0.05$). The TSP-1+MSC group showed superior fracture healing, bone mineralization, trabecular thickness, and bone density compared to the single-treatment TSP-1 and MSC groups ($p < 0.05$). Immunohistochemical analysis revealed that, compared to the model group, the expression of CD105, CD31, and BMP-2 was significantly increased in the TSP-1 and MSC groups ($p < 0.05$), with the TSP-1+MSC group showing higher expression levels than the single treatment groups ($p < 0.05$). Hematoxylin-eosin staining results showed that in the TSP-1 and MSC groups, fibrous tissue was gradually replaced by bone tissue, with mature bone formation observed. The TSP-1+MSC group exhibited more mature bone tissue. *In vitro*, TSP-1 treatment significantly promoted endothelial cell proliferation and tube formation, with higher protein expression levels of COX-2 and VEGF detected as compared to the control group ($p < 0.05$). Additionally, TSP-1 significantly enhanced MSC migration and tube formation, and upregulated the expression of endothelial cell markers CD31, VEGFR1, and VEGFR2 in MSCs ($p < 0.05$).

Conclusions: Both TSP-1 and MSCs, whether used alone or in combination, significantly promoted bone formation and angiogenesis during the fracture healing process. The combined treatment with TSP-1 and MSC showed the most significant effects, suggesting a synergistic role in accelerating fracture repair. These results provide new evidence for the potential applications of TSP-1 and MSCs in bone fracture healing and vascular regeneration.

Keywords: thrombospondin-1; fracture healing; mesenchymal stem cells; angiogenesis

Introduction

Fractures represent a common type of trauma worldwide, especially among the elderly, with the incidence significantly increasing with age [1,2]. Although most fractures can gradually heal through self-repair, complex fractures, fractures in areas with limited blood supply, and fractures accompanied by osteoporosis often experience delayed healing, nonunion, or healing failure [3,4]. These complications cause considerable pain in patients and significantly reduce their quality of life. Fracture healing is a complex biological process that involves inflammation, cartilage and bone tissue regeneration, and angiogenesis [5,6]. Therefore, developing therapeutic strategies that can simultaneously promote osteogenesis and angiogenesis to accelerate fracture healing holds significant clinical importance.

Bone tissue regeneration and angiogenesis are two closely linked biological processes. Angiogenesis provides the necessary nutrients and oxygen for newly formed bone tissue, while the migration and differentiation of osteoblasts are key steps in new bone formation [7,8]. During osteogenesis, insufficient angiogenesis may lead to limited or delayed bone tissue formation, making the promotion of angiogenesis crucial for accelerating fracture repair [9]. Recent years have seen a surge in the adoption of mesenchymal stem cells (MSCs) in bone repair research by virtue of their pluripotency and ability to secrete various growth factors that promote bone tissue regeneration and angiogenesis [10,11]. MSCs can activate osteoblasts and endothelial cells through secreted cytokines and exosomes, enhancing tissue repair at the fracture site [12,13]. However, the recruitment efficiency and differentiation potential of MSCs at injury site remain suboptimal, and optimizing their application continues to pose a challenge in current bone repair research.

In addition to MSCs, thrombospondin-1 (TSP-1), a multifunctional extracellular matrix protein, has gained widespread attention in recent years [14]. TSP-1 plays a critical role in regulating various physiological processes such as angiogenesis, cell migration, and tissue repair [15–17]. Particularly, its role in tissue repair is mediated through the modulation of angiogenesis, which enhances local blood supply to promote tissue regeneration [18]. Unlike conventional angiogenic factors like vascular endothelial growth factor (VEGF), which primarily act through well-characterized pathways (e.g., VEGF/vascular endothelial growth factor receptor 2 (VEGFR2) signaling) to stimulate endothelial proliferation and vessel sprouting, TSP-1 is traditionally considered an anti-angiogenic matricellular protein [19]. However, a recent study has uncovered a more nuanced role of TSP-1, demonstrating its context-dependent pro-angiogenic or modulatory effects, particularly in tissue remodeling and repair [20].

It has been shown that TSP-1 not only exhibits strong pro-angiogenic properties in wound healing but also promotes tissue repair through interactions with other cytokines [17]. Therefore, TSP-1 holds promise in bone tissue regeneration by regulating angiogenesis in the process of fracture healing.

Although the potential of MSCs and TSP-1 in fracture repair has been widely studied, their synergistic mechanisms have not been fully elucidated. Whether TSP-1 can further enhance the osteo-healing effects of MSCs by promoting their migration, engraftment, and vascular differentiation remains insufficiently supported by experimental data. Therefore, a deeper investigation into the synergistic mechanisms of TSP-1 and MSCs in fracture repair is crucial to providing a theoretical foundation for future clinical applications.

This study aims to systematically evaluate the independent and combined effects of TSP-1 and MSCs on fracture healing using a rat femoral fracture model. We hypothesize that TSP-1 can directly promote angiogenesis and further accelerate fracture healing by enhancing MSC migration and vascular differentiation. To test this hypothesis, we analyzed the effects of TSP-1 and MSCs on trabecular formation, bone tissue mineralization, angiogenesis, and osteogenic differentiation, with the goal of uncovering their synergistic mechanisms in fracture repair. Our research not only provides new experimental evidence for the combined use of TSP-1 and MSCs in fracture healing but also offers theoretical guidance for developing more clinically effective therapies for fracture repair.

Materials and Methods

Establishment of a Stable Femoral Fracture Model

Forty male Sprague–Dawley rats (6–8 weeks old, each weighing 200–250 g) were purchased from Charles river (Beijing, China) The rats were anesthetized using isoflurane to ensure complete anesthesia [21]. Hair on the right femur was shaved, and the area was disinfected and covered with a sterile surgical drape.

First, a hole was drilled into the proximal end of the femur, and a 25-gauge needle was inserted through a small incision above the knee joint into the medullary cavity to ensure stabilization after fracture. A microcutter was used to create a transverse or oblique fracture in the midshaft of the femur, ensuring the fracture line was neat and completely broken. The intramedullary needle was then pushed into the distal end of the femur to align and stabilize the two fracture ends.

After surgery, the skin incision was sutured with absorbable sutures to ensure proper wound healing. The 40 rats were randomly divided into four groups using a random number table: model group, TSP-1 group, MSC group, and TSP-1+MSC group. In the TSP-1 group, the rats were subcutaneously injected with human TSP-1 recombinant pro-

tein (10 µg/kg/day). The dosage of TSP-1 was determined based on preliminary experiments conducted in our laboratory. The rats in the MSC group received tail vein injections of bone marrow mesenchymal stem cells (BM-MSCs; 1×10^5 cells). In the TSP-1+MSC group, the rats received both TSP-1 recombinant protein (10 µg/kg/day) subcutaneously and BM-MSCs (1×10^5 cells) via tail vein injection. The rats in the model group were injected with an equivalent volume of saline.

Fourteen days after the fracture, the rats were euthanized via intraperitoneal injection of 3% pentobarbital sodium (110 mg/kg), and the tissues encompassing the femoral fracture healing sites were harvested for analysis of the healing process. This study has been approved by the Beijing Keweite Laboratory Animal Welfare Ethics Committee (approval no. KWT-2023-1221-01).

Micro-Computed Tomography (micro-CT)

Upon collection, the femoral tissue samples collected from the experimental rats were immediately fixed to prevent deformation. After fixation, the samples undergo dehydration through a series of ethanol concentrations until fully dehydrated, and were then stored at –80 °C until scanning. The samples were scanned using a micro-CT scanner with the following parameters: resolution set to 10 µm, a voltage at 40 kV, a current at 200 µA, scanning angle of 360°, and exposure time typically set to 1000 ms. The fixed and dehydrated bone samples were placed on the scanning platform. Layer-by-layer scanning was performed, converting the 2D images into 3D data. Upon scan completion, micro-CT software (SkyScan NRecon, NRecon 1.6.x.x, Bruker microCT, Kontich, Belgium) was used to reconstruct the images, generating a 3D structural representation of the sample for further analysis of various parameters.

Immunohistochemistry

Fracture healing tissues were collected from the rats for immunohistochemical analysis. After fixation, the tissues were dehydrated through a series of ethanol concentrations, embedded in paraffin, and sectioned into 4–6 µm slices. The sections were subjected to dewaxing and rehydration, followed by heat-induced antigen retrieval (HIER). To block endogenous peroxidase activity, the sections were treated with 3% hydrogen peroxide, and nonspecific binding sites were blocked with 5% bovine serum albumin. The sections were incubated with primary antibodies (Cluster of Differentiation 105 (CD105), Cluster of Differentiation 31 (CD31), Bone Morphogenetic Protein-2 (BMP-2)), followed by washing. Afterward, Horseradish Peroxidase (HRP)-conjugated secondary antibodies were applied, and after washing, 3,3′-Diaminobenzidine (DAB) chromogen was used for color development for 5 minutes. Hematoxylin was used for counterstaining to visualize cell nuclei. Finally, the sections were dehydrated with ethanol, cleared with xylene, and mounted with a coverslip. Stained tissue sections were examined under a microscope, and quantitative analysis was performed using ImageJ software (version1.5f, NIH, Bethesda, MD, USA).

Hematoxylin-Eosin (HE) Staining

The tissue was fixed and dehydrated through a series of increasing ethanol concentrations. Xylene was used for clearing. The tissue was embedded in paraffin and sectioned into 4–6 µm slices. The sections were dewaxed and hydrated using decreasing concentrations of ethanol, prior to staining with hematoxylin for 10 minutes. After washing, eosin staining was performed for 3 minutes, followed by washing. The sections were dehydrated through a series of ethanol concentrations and cleared with xylene. After a mounting medium was applied, the cleared sections were covered with a coverslip, gently pressed, and allowed to dry. The stained sections were observed under a microscope to analyze the tissue and cellular structure.

Cell Culture

Human umbilical vein endothelial cells (HUVECs; iCell-h110) were purchased from iCELL (Shanghai, China). Endothelial cell-specific culture medium was used. HUVECs were cultured in an incubator at 37 °C with 5% CO_2. The culture medium was changed every 3 days, and when the cells reached 80%–90% confluence, they were trypsinized and passaged. Rat BM-MSCs (RAT-iCell-s018), purchased from iCELL, were cultured in Dulbecco's Modified Eagle Medium (DMEM) containing 10% fetal bovine serum. The cells were cultured in an incubator at 37 °C with 5% CO_2. The culture medium was replaced when the cells reached 70%–80% confluence, followed by enzymatic digestion and subculturing. The HUVECs used had been authenticated by means of STR approach, whereas the BM-MSCs had been subjected to species identification. All cells tested negative for mycoplasma contamination.

Cell Treatment

HUVECs were randomly divided into two groups: control group and TSP-1 group (10 nM). The dosage of TSP-1 was determined based on preliminary experiments conducted in our laboratory. Similarly, MSCs were also randomly divided into two groups: control group and TSP-1 group (100 nM).

5-ethynyl-2′-deoxyuridine (EdU) Staining

Click-iT EdU kit (C10337, Thermo Fisher Scientific, Waltham, MA, USA) was used for EdU staining. Cell culture medium supplemented with EdU was added to cells for a 1-hour incubation. After the medium was removed, the cells were fixed and then washed. The cells were permeabilized using a permeabilization agent. A reaction mixture, prepared according to the kit instructions, was added to the cells for a 30-minute incubation. After washing, 4′6-

diamidino-2-phenylindole (DAPI) staining (C1006, Beyotime, Shanghai, China) was performed for 5 minutes to visualize the nuclei. Following washing, EdU-positive cells were observed using a fluorescence microscope (BX53, Olympus, Tokyo, Japan).

Western Blotting

The harvested cells were first treated with lysis buffer to obtain protein samples. The samples were mixed with sodium dodecyl sulfate (SDS) sample buffer (ST626, Beyotime, Shanghai, China) and then boiled to achieve protein denaturation. Next, the proteins were separated using sodium dodecyl sulfate–polyacrylamide gel electrophoresis (SDS-PAGE) based on their molecular weight. Afterward, the separated proteins were transferred from the gel to a polyvinylidene fluoride (PVDF) membrane (FFP19, Beyotime, Shanghai, China). Once transferred, nonspecific binding sites on the membrane were blocked using a blocking solution. Then, the membrane was incubated with a diluted primary antibody overnight at 4 °C or at room temperature, followed by washing with TBS with Tween-20 (TBST) (J77500.K8, Thermo Fisher Scientific, Waltham, MA, USA). Among the tested primary antibodies are cyclooxygenase-2 (COX-2) (1:1000, ab179800, Abcam, Cambridge, UK) and vascular endothelial growth factor A (VEGF-A) (1:1000, ab46154, Abcam, Cambridge, UK). After that, the membrane was incubated with an HRP-conjugated secondary antibody (1:1000, ab6721, Abcam, Cambridge, UK). Finally, after washing, enhanced chemiluminescence (ECL) (P0018S, Beyotime, Shanghai, China) chemiluminescent substrate was added and the emitted signals were detected using a gel imaging system. The protein expression levels were quantified using ImageJ software (version 1.5f, NIH, Bethesda, MD, USA).

Tube Formation Assay

An appropriate amount of Matrigel was added to cover the entire bottom of a 24-well plate. The plate was then placed in a 37 °C incubator for 30 minutes to allow the Matrigel to solidify into a gel. The cultured endothelial cells or MSCs were seeded at a density of 1×10^5 cells/well onto the solidified Matrigel. Then, the cells were incubated in an incubator for 24 hours under conditions suitable for cell growth. To induce tube formation, VEGF (20 ng/mL) was added to the culture medium. After 24 hours, the cell morphology was observed under a microscope. Tube formation length was quantified using ImageJ software (version 1.5f, NIH, Bethesda, MD, USA).

Transwell Assay

First, the cells to be tested was resuspended in culture medium, generally at a concentration of 1×10^5 cells/mL. Then, an appropriate amount of culture medium (containing 10% fetal bovine serum) was added to the lower chamber of the Transwell insert, and 100 µL of the cell suspension was added to the upper chamber. The insert was placed into a 24-well plate and incubated for 24 hours, allowing the cells to migrate through the membrane pores to the lower chamber. After incubation, the upper chamber was washed with phosphate-buffered saline (PBS) to remove non-migrated cells, and the upper surface of the Transwell insert was gently wiped. Next, the insert was immersed in fixative for 10 minutes, wash, and stained with crystal violet solution for 10 minutes; subsequently, excess dye was washed away. Finally, the migrated cells on the lower surface of the membrane were observed under a microscope. The migrated cells were enumerated using ImageJ software (version 1.5f, NIH, Bethesda, MD, USA).

Immunofluorescence (IF) Staining

Firstly, cell smears of the treated MSCs were prepared and then fixed for 15 minutes. After washing with PBS, the cells were permeabilized using a permeabilizing agent for 10 minutes, followed by washing. Then, non-specific binding sites were blocked by incubating the cells with 5% skim milk for 30 minutes. Afterward, the cell smears were incubated overnight at room temperature with diluted primary antibodies against CD31 (1:1000, ab9498, Abcam, Cambridge, UK), vascular endothelial growth factor receptor 1 (VEGFR1) (1:1000, ab2350, Abcam, Cambridge, UK), and VEGFR2 (1:1000, ab234110, Abcam, Cambridge, UK). After incubation, the samples were washed and fluorescence-labeled secondary antibodies (1:1000, ab175702, ab150080, Abcam, Cambridge, UK) were applied for a 1-hour incubation, followed by another wash. Then, the cell nuclei were stained with DAPI for 10 minutes, followed by washing. Finally, the samples were mounted with mounting medium and observed using a fluorescence microscope. The expression levels of CD31, VEGFR1, and VEGFR2, along with their fluorescence intensities, were quantified using ImageJ software (version 1.5f, NIH, Bethesda, MD, USA).

Statistical Analysis

Statistical analysis was conducted using GraphPad Prism software (version 9.0, GraphPad Software Inc., San Diego, CA, USA). The data were analyzed using *t*-tests and one-way analysis of variance (ANOVA), followed by Tukey's post-hoc test for multiple comparisons. Results are presented as mean ± standard deviation (SD). A p-value of less than 0.05 was considered statistically significant.

Results

TSP-1 and/or MSC Treatment Promotes Fracture Healing in Rat Femur

Two weeks post-surgery, tissue at the fracture callus site was observed using micro-CT. Compared to the model group, the TSP-1 and MSC groups showed significantly more callus, denser trabecular bone, and higher levels of

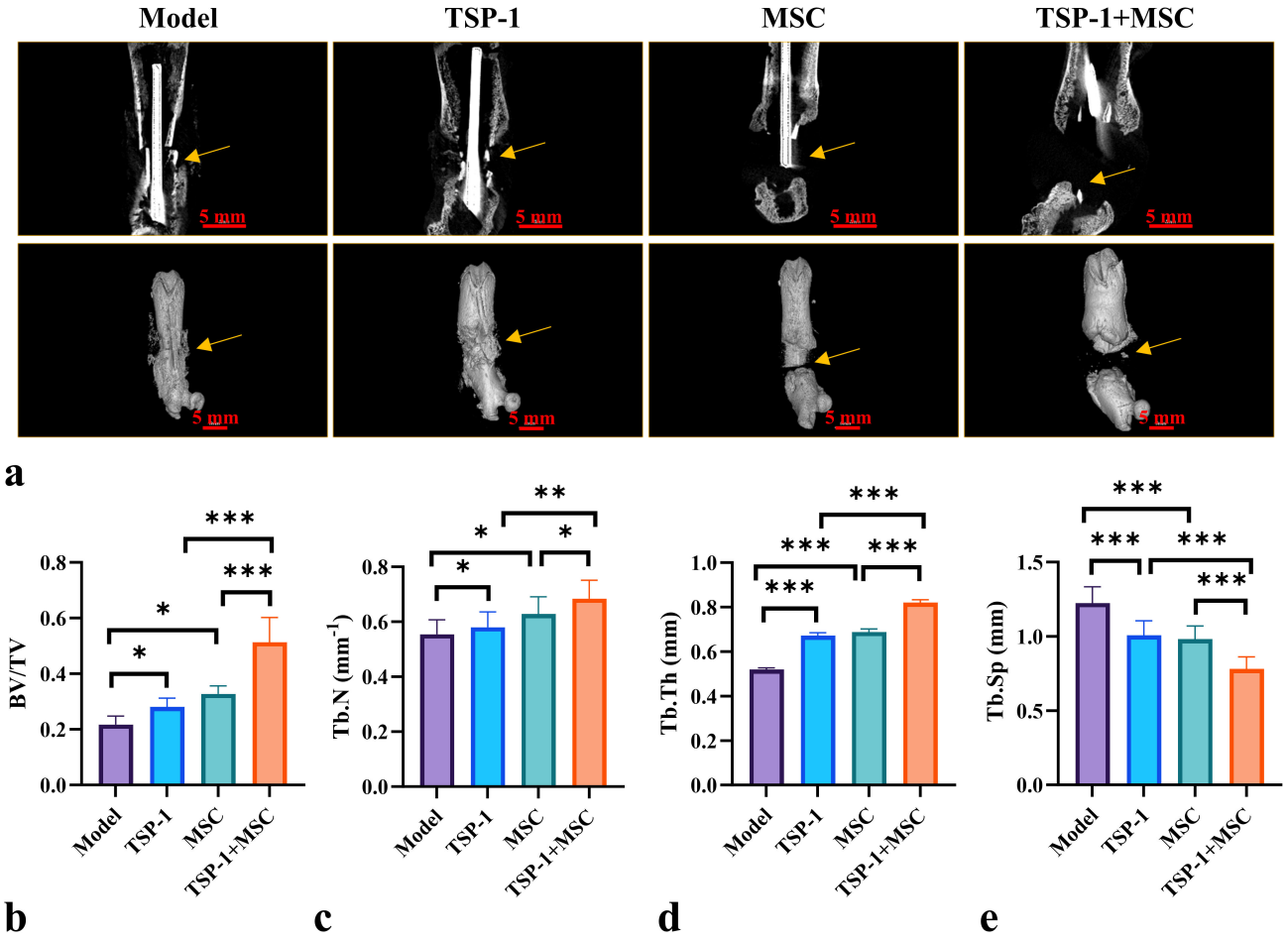

Fig. 1. TSP-1 and/or MSC treatment promotes fracture healing in rat femur. (a) micro-CT images of the trabecular bone in the proximal femur fracture site of rat. The arrow indicates the area of new callus formation. (b) Measurement of bone volume over total volume (BV/TV). (c) Evaluation of trabecular number (Tb.N). (d) Quantitative analysis of trabecular thickness (Tb.Th) via micro-CT. (e) Assessment of trabecular separation (Tb.Sp). $n = 10$. * $p < 0.05$, ** $p < 0.01$, *** $p < 0.001$. Abbreviations: MSC, mesenchymal stem cell; TSP-1, thrombospondin-1; micro-CT, micro-computed tomography.

mineralization. The TSP-1+MSC group exhibited even greater levels of fracture healing and mineralization compared to the TSP-1 and MSC groups (Fig. 1a). Compared to the model group, the TSP-1 and MSC groups showed significant increases in trabecular thickness, trabecular number, and bone mineral density ($p < 0.05$) (Fig. 1b–e). Additionally, the treatment combining TSP-1 and MSC led to more pronounced increases in trabecular thickness, trabecular number, and bone mineral density compared to the single treatments of TSP-1 and MSC ($p < 0.05$) (Fig. 1b–e). In contrast, compared to the model group, both the TSP-1 and MSC groups exhibited significantly reduction in trabecular separation ($p < 0.05$), whereas the combined treatment with TSP-1 and MSC led to a more significant reduction in trabecular separation ($p < 0.05$) (Fig. 1b–e).

TSP-1 and/or MSC Treatment Promotes Angiogenesis and Osteogenesis During Fracture Healing

We assessed the expression of CD105, CD31, and BMP-2 in the callus tissue via immunohistochemistry. The results revealed that, compared to the model group, the TSP-1 and MSC groups showed significantly increased expression of CD105, CD31, and BMP-2 (Fig. 2a–f) ($p < 0.05$). Furthermore, the expression of CD105, CD31, and BMP-2 in the TSP-1+MSC group was significantly higher than in the TSP-1 and MSC groups ($p < 0.05$). According to the HE staining results, the model group exhibited partial fibrous and cartilage tissue but no mature bone tissue (Fig. 2g). In the TSP-1 and MSC groups, fibrous tissue was gradually replaced by bone tissue, with some mature bone observed. In contrast, more mature bone tissue was observed in the TSP-1+MSC group.

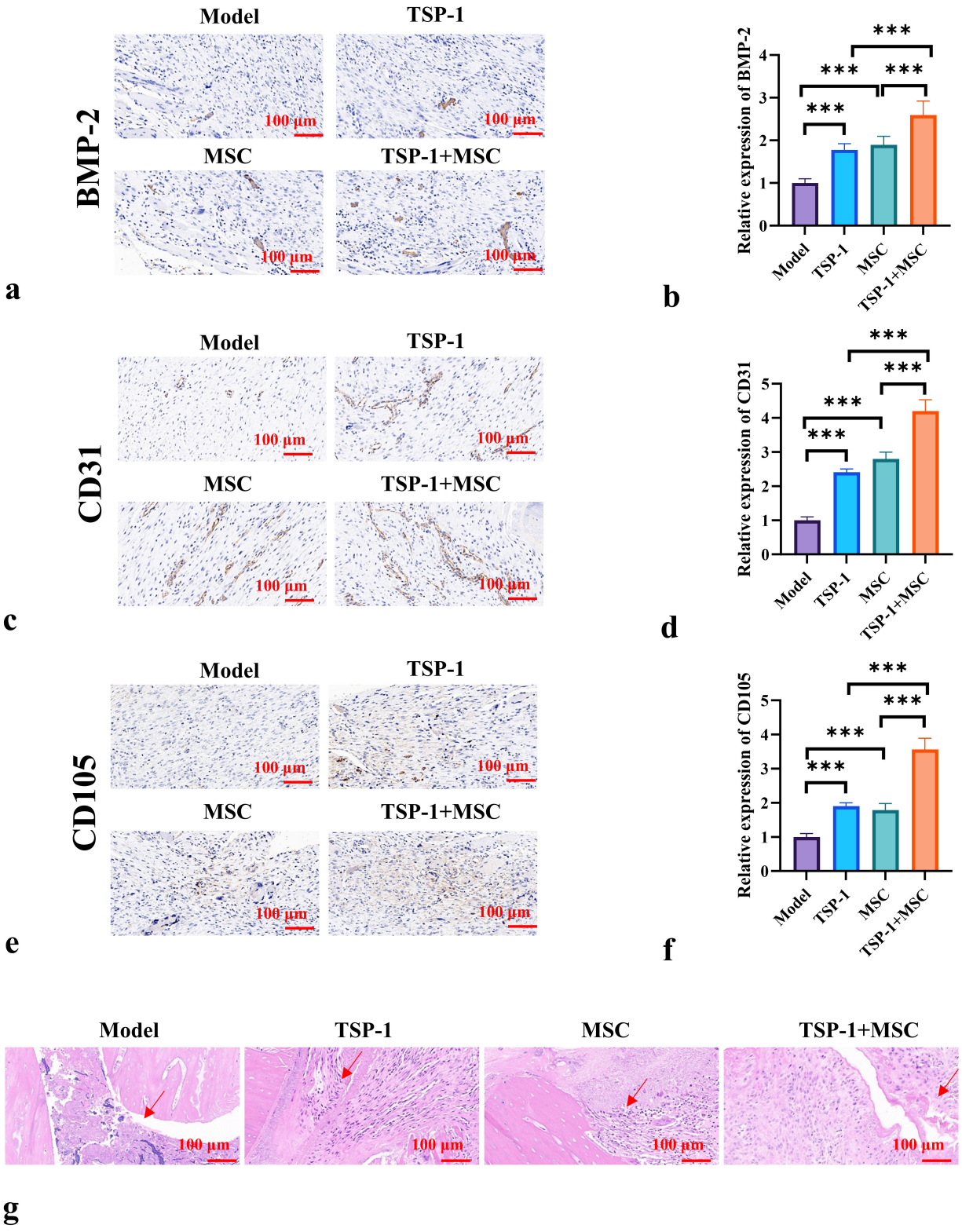

Fig. 2. TSP-1 and/or MSC treatment promotes angiogenesis and osteogenesis during fracture healing. (a,b) IHC analysis of Bone Morphogenetic Protein-2 (BMP-2) expression in fracture healing tissue of rat after TSP-1 and/or MSC treatment. (c,d) IHC analysis of Cluster of Differentiation 31 (CD31) expression in fracture healing tissue of rat after TSP-1 and/or MSC treatment. (e,f) IHC analysis of Cluster of Differentiation 105 (CD105) expression in fracture healing tissue of rat after TSP-1 and/or MSC treatment. (g) HE staining of fracture healing tissue in rat. The arrow indicates the area of newly formed bone tissue. $n = 10$. *** $p < 0.001$. Abbreviations: HE, hematoxylin-eosin; IHC, immunohistochemistry; MSC, mesenchymal stem cell; TSP-1, thrombospondin-1.

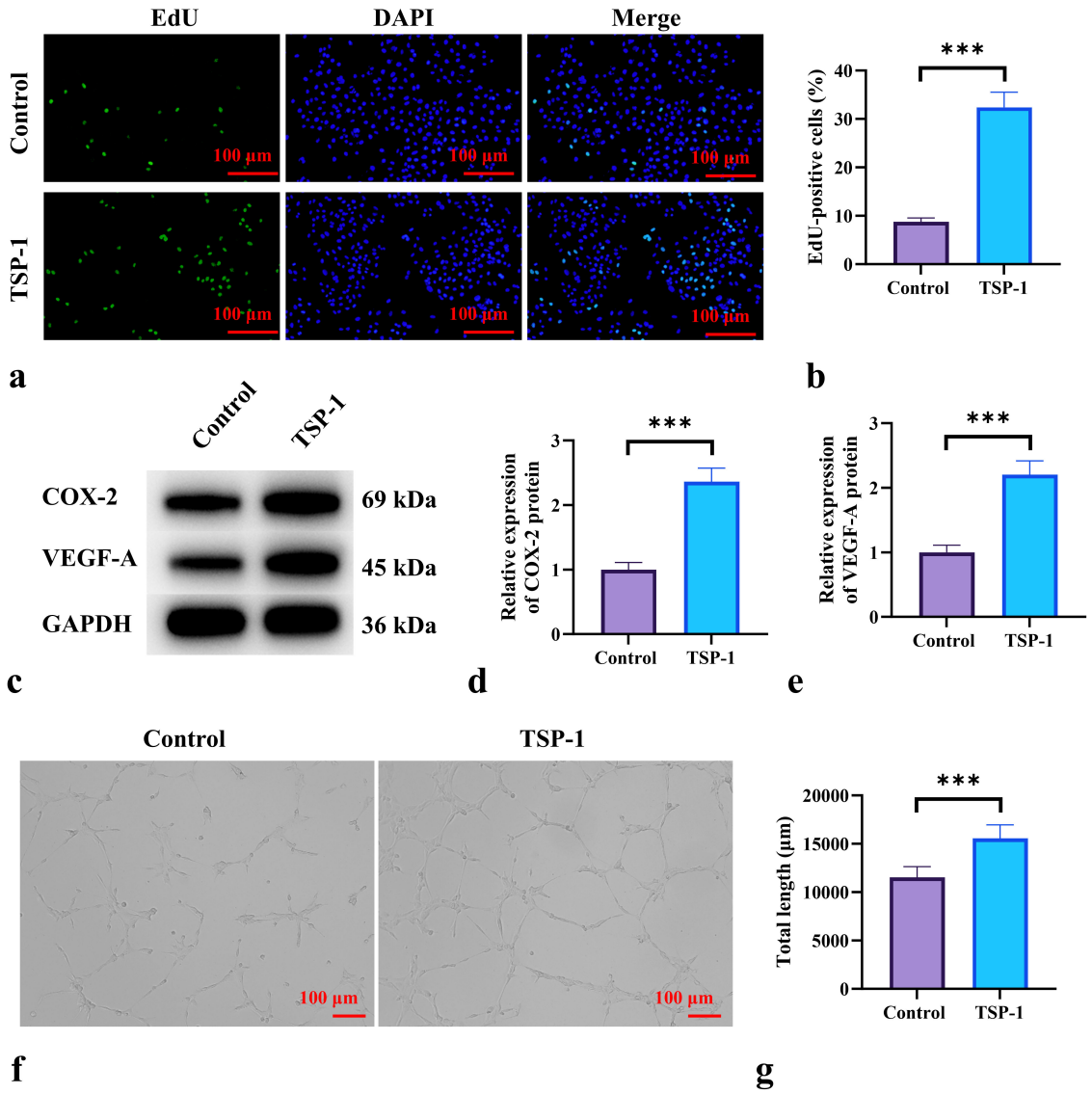

Fig. 3. TSP-1 treatment directly increases endothelial cell proliferation and tube formation *in vitro*. (a,b) EdU staining results depicting the effect of TSP-1 on HUVEC proliferation. (c–e) Western blot analysis of COX-2 and VEGF-A protein expression in HUVECs. (f,g) Tube formation assay results depicting the effect of TSP-1 on HUVEC tube formation. $n = 6$. *** $p < 0.001$. Abbreviations: HUVEC, human umbilical vein endothelial cell; TSP-1, thrombospondin-1; VEGF-A, vascular endothelial growth factor A; EdU, 5-ethynyl-2′-deoxyuridine; COX-2, cyclooxygenase-2; DAPI, 4′6-diamidino-2-phenylindole; GAPDH, glyceraldehyde 3-phosphate dehydrogenase.

TSP-1 Treatment Directly Increases Endothelial Cell Proliferation and Tube Formation In Vitro

To investigate the mechanism by which TSP-1 enhances angiogenesis during bone healing, we first performed EdU staining to assess endothelial cell proliferation after TSP-1 treatment. The results showed that the number of EdU-positive endothelial cells was significantly higher in the TSP-1 group compared to the control group ($p < 0.05$) (Fig. 3a,b). We also measured the protein expression levels of COX-2 and VEGF in endothelial cells. The results revealed that the protein expression levels of COX-2 and VEGF in TSP-1-treated endothelial cells were significantly higher than in the control group (Fig. 3c–e) ($p < 0.05$). Furthermore, the results of the tube formation assay showed that the number and length of tube formations were significantly increased in TSP-1-treated endothelial cells compared to the control group (Fig. 3f,g) ($p < 0.05$).

TSP-1 Enhances Angiogenesis Indirectly by Promoting MSC Migration and Vascular Differentiation

Our study demonstrated that TSP-1 was able to recruit MSCs and significantly increased tube formation in MSCs *in vitro*. After co-incubating MSCs with TSP-1 for 7 days,

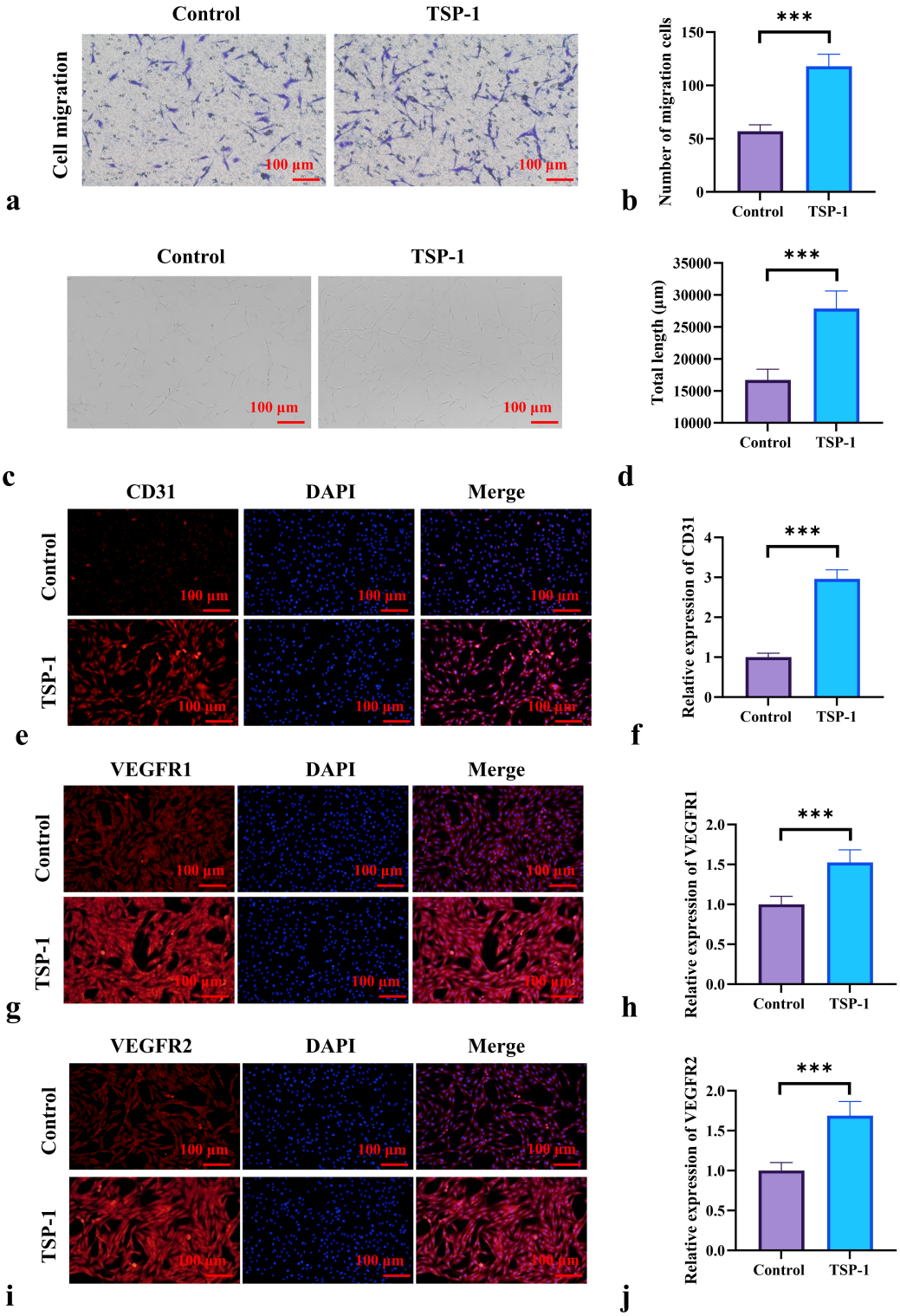

Fig. 4. TSP-1 enhances angiogenesis indirectly by promoting MSC migration and vascular differentiation. (a,b) Transwell assay results showing the effect of TSP-1 on MSC migration. (c,d) Tube formation assay results showing the effect of TSP-1 on MSC tube formation. (e,f) IF analysis of the effect of TSP-1 on CD31 expression in MSCs. (g,h) IF analysis of the effect of TSP-1 on VEGFR1 expression in MSCs. (i,j) IF analysis of the effect of TSP-1 on VEGFR2 expression in MSCs. $n = 6$, *** $p < 0.001$. Abbreviations: MSC, mesenchymal stem cell; TSP-1, thrombospondin-1; IF, immunofluorescence; VEGFR1, vascular endothelial growth factor receptor 1; VEGFR2, vascular endothelial growth factor receptor 2; CD31, Cluster of Differentiation 31; DAPI, 4′6-diamidino-2-phenylindole.

results from the Transwell migration assays showed that TSP-1 significantly promoted MSC migration ($p < 0.05$) (Fig. 4a,b). The tube formation assay further demonstrated that TSP-1 promoted tube formation of MSCs *in vitro* ($p < 0.05$) (Fig. 4c,d). Additionally, IF results showed that the expression of endothelial cell markers CD31, VEGFR1, and VEGFR2 was significantly upregulated in MSCs compared to the control group (Fig. 4e–j). These findings confirm that TSP-1 indirectly promotes initial angiogenesis by enhancing MSC migration and differentiation into endothelial-like cells.

Discussion

In this study, we comprehensively assessed the individual and synergistic effects of TSP-1 and MSCs on bone healing using a rat femoral fracture model. Our findings demonstrated that both TSP-1 and MSCs independently promoted fracture healing and, when combined, further enhanced the formation of both bone and blood vessels. These results contribute to a deeper understanding of the mechanisms underlying bone repair and offer new insights and potential strategies for fracture treatment. To provide a broader context for these findings, we provide a multifaceted comparative analysis of our findings with other relevant studies in the following.

This study showed that TSP-1 treatment significantly enhanced trabecular bone density, mineralization, and angiogenesis at the fracture site, primarily by promoting endothelial cell proliferation and blood vessel formation, thereby accelerating healing. These findings align with the research by Pourheydar *et al*. [22], which demonstrated that TSP-1 boosts angiogenesis through the activation of COX-2 and VEGF signaling pathways. In our study, we also observed a marked increase in COX-2 and VEGF expression in endothelial cells treated with TSP-1, and the EdU proliferation assay confirmed that TSP-1 effectively promoted endothelial cell proliferation. Bardag-Gorce *et al*.'s work [23] further underscores the dual role of TSP-1 in tissue repair and angiogenesis, providing solid support for our results.

Moreover, TSP-1 not only directly promotes angiogenesis but also further enhances vascularization by facilitating MSC migration and differentiation. This is consistent with the findings of Tietze *et al*. [24], who studied the role of TSP-1 in MSC recruitment and migration. Our study confirmed the promoting effect of TSP-1 on MSC migration through Transwell assays and demonstrated MSC differentiation into endothelial-like cells via IF. These results suggest that TSP-1 not only acts directly on endothelial cells but also indirectly influences the angiogenic potential of MSCs, thereby contributing more comprehensively to fracture healing.

The role of MSCs in bone repair has been widely recognized, particularly in the context of angiogenesis and osteogenic differentiation during fracture healing. A study by Guillamat-Prats [25] demonstrated that MSCs promote the generation of new blood vessels and enhance bone tissue regeneration by secreting a variety of growth factors and cytokines. In our study, the MSC treatment group also significantly increased trabecular bone density and mineralization, while the expression of vascular and osteogenic markers such as CD105, CD31, and BMP-2 was notably enhanced. These findings align with the results of Bian *et al*. [26], further confirming that MSCs play a crucial role in bone and vascular generation through their secretory activity. The synergistic effect may be attributed to TSP-1 enhancing the paracrine activity of MSCs.

Additionally, MSCs further promote angiogenesis and bone healing at the fracture site through interactions with endothelial cells. A study by Zhang *et al*. [27] indicated that MSCs can accelerate bone repair by secreting exosomes and angiogenic factors, such as VEGF, which promote angiogenesis in collaboration with endothelial cells. Our study similarly demonstrated that MSCs not only enhanced osteogenic differentiation but also, in combination with TSP-1, significantly enhanced the angiogenic capacity of endothelial cells. This further underscores that MSCs are not only functionally involved in osteogenesis during bone repair but also engage in the synergistic regulation of angiogenesis.

Notably, the combination of TSP-1 and MSCs in this study exhibited a significant synergistic effect. Compared to the use of TSP-1 or MSCs alone, the TSP-1+MSC treatment significantly increased trabecular thickness, number, density, and mineralization, with a marked upregulation in the expression of markers such as CD105, CD31, and BMP-2. This finding is consistent with the results of Gong *et al*. [28], who demonstrated that MSCs, in synergy with TSP-1, accelerate angiogenesis at the fracture site and promote bone tissue regeneration by enhancing extracellular matrix remodeling.

The results of this study are consistent with numerous studies concerning TSP-1 and MSCs in bone repair, while also expanding the understanding of their synergistic mechanisms in fracture healing. Luo *et al*. [29] suggested that TSP-1 plays an important role in the early stages of bone healing by regulating immune responses and enhancing angiogenesis. Our study further validates this perspective, showing that TSP-1 can enhance angiogenesis at the fracture site through both direct and indirect mechanisms, and accelerate bone repair through its synergistic action with MSCs.

Furthermore, this study is the first to demonstrate that TSP-1 indirectly enhances angiogenesis by promoting the differentiation of MSCs into endothelial-like cells. This finding provides new directions for future bone repair therapeutic strategies and offers experimental evidence for the application of TSP-1 and MSCs in regenerative medicine.

Although this study has made important discoveries, there are still some limitations. Firstly, this study was limited to a rat model, and the actual effects in clinical applications need to be further validated. Additionally, the mechanisms of action of TSP-1 and MSCs in bone repair are complex, and future research could further explore their specific roles in immune regulation, inflammatory responses (such as failure to detect interleukin (IL)-6/tumor necrosis factor α (TNF-α)), and extracellular matrix remodeling. Although recombinant BMP-2 is widely used clinically as an osteoinductive factor, its clinical application remains constrained by several limitations. For example, supraphysiological doses are often required to achieve therapeutic efficacy, which can lead to complications such as ectopic bone formation, inflammatory responses, and even an increased risk of tumor development in some cases. In addition, the high cost and short biological half-life of BMP-2 further limit its clinical utility. In contrast, our study demonstrates that the combined treatment with TSP-1 and MSCs exhibits superior efficacy and potentially enhanced safety.

Future studies could integrate gene editing technologies to clarify the specific signaling pathways through which TSP-1 regulates MSC migration and differentiation, and explore how gene modulation can optimize the therapeutic effects of TSP-1 and MSCs. Furthermore, based on the findings of this study, clinical trials can be organized to explore the potential application of combined treatment with TSP-1 and MSC in complex fractures and chronic bone injuries.

Conclusions

This study aims to evaluate the role of TSP-1 and MSCs in fracture healing using a rat femoral fracture model and investigate their synergistic effects in promoting bone tissue regeneration and angiogenesis. Both TSP-1 and MSCs can independently enhance trabecular formation, mineralization, and vascularization, and their combined application further amplifies bone and vascular formation at the fracture site. This synergistic effect is primarily mediated by TSP-1's direct involvement in promoting endothelial cell proliferation and angiogenesis, as well as its indirect enhancement of angiogenesis through MSC migration and differentiation. Additionally, the combined treatment with TSP-1 and MSCs drives the maturation of bone tissue and osteogenic differentiation, providing a potential strategy for fracture repair.

These findings offer new insights into the application of TSP-1 and MSCs in bone repair and lay the foundation for future research on fracture treatments. Based on our current findings in a rat model, further clinical studies are warranted to assess their potential in promoting fracture healing in humans. This study provides valuable experimental evidence for the future development of regenerative medical therapies based on TSP-1 and MSCs.

Availability of Data and Materials

The data that support the findings of this study are available from the corresponding author upon reasonable request.

Author Contributions

CBW, XL and XLZ designed the research study. CBW has been involved in drafting the manuscript. CBW performed the research. CBW and XL provided help and advice on the experiments. XLZ analyzed the data. All authors contributed to important editorial changes in the manuscript. All authors read and approved the final manuscript. All authors have participated sufficiently in the work and agreed to be accountable for all aspects of the work.

Ethics Approval and Consent to Participate

The study has been approved by the Beijing Keweite Laboratory Animal Welfare Ethics Committee (approval No. KWT-2023-1221-01).

Acknowledgment

Not applicable.

Funding

This research received no external funding.

Conflict of Interest

The authors declare no conflict of interest.

References

[1] Vlachos C, Ampadiotaki MM, Papagrigorakis E, Galanis A, Zachariou D, Vavourakis M, *et al*. Distinctive Geometrical Traits of Proximal Femur Fractures-Original Article and Review of Literature. Medicina (Kaunas, Lithuania). 2023; 59: 2131. https://doi.org/10.3390/medicina59122131.

[2] Nauth A, Haller J, Augat P, Anderson DD, McKee MD, Shearer D, *et al*. Distal femur fractures: basic science and international perspectives. OTA International: the Open Access Journal of Orthopaedic Trauma. 2024; 7: e320. https://doi.org/10.1097/OI9.0000000000000320.

[3] Gurung R, Terrill A, White G, Windolf M, Hofmann-Fliri L, Dlaska C, *et al*. Severity of Complications after Locking Plate Osteosynthesis in Distal Femur Fractures. Journal of Clinical Medicine. 2024; 13: 1492. https://doi.org/10.3390/jcm13051492.

[4] Chandran M, Akesson KE, Javaid MK, Harvey N, Blank RD, Brandi ML, *et al*. Impact of osteoporosis and osteoporosis medications on fracture healing: a narrative review. Osteoporosis International: a Journal Established as Result of Cooperation between the European Foundation for Osteoporosis and the National Osteoporosis Foundation of the USA. 2024; 35: 1337–1358. https://doi.org/10.1007/s00198-024-07059-8.

[5] Ehnert S, Histing T. Advances in Fracture Healing Research. Bioengineering (Basel, Switzerland). 2024; 11: 67. https://doi.org/10.3390/bioengineering11010067.

[6] Zou NY, Liu R, Huang M, Jiao YR, Wei J, Jiang Y, *et al*. Age-related secretion of grancalcin by macrophages induces skeletal stem/progenitor cell senescence during fracture healing. Bone Research. 2024; 12: 6. https://doi.org/10.1038/s41413-023-00309-1.

[7] Zha K, Hu W, Xiong Y, Zhang S, Tan M, Bu P, *et al*. Nanoarchitecture-Integrated Hydrogel Boosts Angiogenesis-Osteogenesis-Neurogenesis Tripling for Infected Bone Fracture Healing. Advanced Science (Weinheim, Baden-Wurttemberg, Germany). 2024; 11: e2406439. https://doi.org/10.1002/advs.202406439.

[8] van Brakel F, Zhao Y, van der Eerden BCJ. Fueling recovery: The importance of energy coupling between angiogenesis and osteogenesis during fracture healing. Bone Reports. 2024; 21: 101757. https://doi.org/10.1016/j.bonr.2024.101757.

[9] Wu Z, Yang Y, Wang M. Silencing p75NTR regulates osteogenic differentiation and angiogenesis of BMSCs to enhance bone healing in fractured rats. Journal of Orthopaedic Surgery and Research. 2024; 19: 192. https://doi.org/10.1186/s13018-024-04653-8.

[10] Yang K, Luan YY, Wang S, Yan YS, Wang YP, Wu J, *et al*. SGMS1 facilitates osteogenic differentiation of MSCs and strengthens osteogenesis-angiogenesis coupling by modulating Cer/PP2A/Akt pathway. iScience. 2024; 27: 109358. https://doi.org/10.1016/j.isci.2024.109358.

[11] Xiao Y, Xie X, Chen Z, Yin G, Kong W, Zhou J. Advances in the roles of ATF4 in osteoporosis. Biomedicine & Pharmacotherapy = Biomedecine & Pharmacotherapie. 2023; 169: 115864. https://doi.org/10.1016/j.biopha.2023.115864.

[12] Farabi B, Roster K, Hirani R, Tepper K, Atak MF, Safai B. The Efficacy of Stem Cells in Wound Healing: A Systematic Review. International Journal of Molecular Sciences. 2024; 25: 3006. https://doi.org/10.3390/ijms25053006.

[13] Gou Y, Huang Y, Luo W, Li Y, Zhao P, Zhong J, *et al*. Adipose-derived mesenchymal stem cells (MSCs) are a superior cell source for bone tissue engineering. Bioactive Materials. 2023; 34: 51–63. https://doi.org/10.1016/j.bioactmat.2023.12.003.

[14] Wu W, Zhao Z, Wang Y, Liu M, Zhu G, Li L. Mechanism research of elastic fixation promoting fracture healing based on proteomics and fracture microenvironment. Bone & Joint Research. 2024; 13: 559–572. https://doi.org/10.1302/2046-3758.1310.BJR-2023-0257.R2.

[15] Pitru A, Gheorghe DN, Popescu DM, Nicolae FM, Boldeanu MV, Turcu-Stiolica A, *et al*. Expression of Vascular Adhesion Protein-1 and Thrombospondin-1 in Gingival Crevicular Fluid of Patients with Periodontitis and Non-Alcoholic Fatty Liver Disease. Journal of Inflammation Research. 2024; 17: 5427–5437. https://doi.org/10.2147/JIR.S448963.

[16] Hu H, Ma J, Peng Y, Feng R, Luo C, Zhang M, *et al*. Thrombospondin-1 Regulates Trophoblast Necroptosis via NEDD4-Mediated Ubiquitination of TAK1 in Preeclampsia. Advanced Science (Weinheim, Baden-Wurttemberg, Germany). 2024; 11: e2309002. https://doi.org/10.1002/advs.202309002.

[17] Lu YZ, Nayer B, Singh SK, Alshoubaki YK, Yuan E, Park AJ, *et al*. CGRP sensory neurons promote tissue healing via neutrophils and macrophages. Nature. 2024; 628: 604–611. https://doi.org/10.1038/s41586-024-07237-y.

[18] Yang X, Zhao H, Li R, Chen Y, Xu Z, Shang Z. Stromal thrombospondin 1 suppresses angiogenesis in oral submucous fibrosis. International Journal of Oral Science. 2024; 16: 17. https://doi.org/10.1038/s41368-024-00286-z.

[19] Ju Y, Tang Z, Dai X, Gao H, Zhang J, Liu Y, *et al*. Protection against light-induced retinal degeneration via dual anti-inflammatory and anti-angiogenic functions of thrombospondin-1. British Journal of Pharmacology. 2022; 179: 1938–1961. https://doi.org/10.1111/bph.15303.

[20] Liu B, Yang H, Song YS, Sorenson CM, Sheibani N. Thrombospondin-1 in vascular development, vascular function, and vascular disease. Seminars in Cell & Developmental Biology. 2024; 155: 32–44. https://doi.org/10.1016/j.semcdb.2023.07.011.

[21] Shpetko YY, Filippenkov IB, Denisova AE, Stavchansky VV, Gubsky LV, Limborska SA, *et al*. Isoflurane Anesthesia's Impact on Gene Expression Patterns of Rat Brains in an Ischemic Stroke Model. Genes. 2023; 14: 1448. https://doi.org/10.3390/genes14071448.

[22] Pourheydar B, Biabanghard A, Azari R, Khalaji N, Chodari L. Exercise improves aging-related decreased angiogenesis through modulating VEGF-A, TSP-1 and p-NF-Kb protein levels in myocardiocytes. Journal of Cardiovascular and Thoracic Research. 2020; 12: 129–135. https://doi.org/10.34172/jcvtr.2020.21.

[23] Bardag-Gorce F, Hoffman C, Meepe I, Ferrini M, Hoft RH, Oliva J, *et al*. Thrombospondin-1 induction and VEGF reduction by proteasome inhibition. Heliyon. 2023; 9: e13397. https://doi.org/10.1016/j.heliyon.2023.e13397.

[24] Tietze L, Christ M, Yu J, Stock P, Nickel S, Schulze A, *et al*. Approaching Thrombospondin-1 as a Potential Target for Mesenchymal Stromal Cells to Support Liver Regeneration after Partial Hepatectomy in Mouse and Humans. Cells. 2024; 13: 529. https://doi.org/10.3390/cells13060529.

[25] Guillamat-Prats R. The Role of MSC in Wound Healing, Scarring and Regeneration. Cells. 2021; 10: 1729. https://doi.org/10.3390/cells10071729.

[26] Bian D, Wu Y, Song G, Azizi R, Zamani A. The application of mesenchymal stromal cells (MSCs) and their derivative exosome in skin wound healing: a comprehensive review. Stem Cell Research & Therapy. 2022; 13: 24. https://doi.org/10.1186/s13287-021-02697-9.

[27] Zhang Y, Liu J, Zou T, Qi Y, Yi B, Dissanayaka WL, *et al*. DPSCs treated by TGF-β1 regulate angiogenic sprouting of three-dimensionally co-cultured HUVECs and DPSCs through VEGF-Ang-Tie2 signaling. Stem Cell Research & Therapy. 2021; 12: 281. https://doi.org/10.1186/s13287-021-02349-y.

[28] Gong M, Wang M, Xu J, Yu B, Wang YG, Liu M, *et al*. Nano-Sized Extracellular Vesicles Secreted from GATA-4 Modified Mesenchymal Stem Cells Promote Angiogenesis by Delivering Let-7 miRNAs. Cells. 2022; 11: 1573. https://doi.org/10.3390/cells11091573.

[29] Luo Q, Jiang Z, Jiang J, Wan L, Li Y, Huang Y, *et al*. Tsp-1^{+} microglia attenuate retinal neovascularization by maintaining the expression of Smad3 in endothelial cells through exosomes with decreased miR-27a-5p. Theranostics. 2023; 13: 3689–3706. https://doi.org/10.7150/thno.84236.